





Warming hiatus and evergreen conifers in Altay-Sayan Region, Siberia

Viacheslav I. KHARUK^{1,2*}  <http://orcid.org/0000-0003-4736-0655>;  e-mail: viharuk@ksc.krasn.ru

Sergei T. IM^{1,2,3}  <http://orcid.org/0000-0002-5794-7938>; e-mail: stim@ksc.krasn.ru

Il'ya A. PETROV¹  <http://www.orcid.org/0000-0002-6652-9594>; e-mail: petrovilsoran@gmail.com

* Corresponding author

¹ Sukachev Institute of Forest, Federal Scientific Center, Russian Academy of Science, Siberian Branch, Akademgorodok 50/28, Krasnoyarsk 660036, Russia

² Siberian Federal University, Svobodny str.79, Krasnoyarsk 660041, Russia

³ Reshetnev Siberian State University of Science and Technology, Krasnoyarsky rabochy str. 31, Krasnoyarsk 660014, Russia

Citation: Kharuk VI, Im ST, Petrov IA (2018) Warming hiatus and evergreen conifers in Altay-Sayan Region, Siberia. *Journal of Mountain Science* 15(12). <https://doi.org/10.1007/s11629-018-5071-6>

© Science Press, Institute of Mountain Hazards and Environment, CAS and Springer-Verlag GmbH Germany, part of Springer Nature 2018

Abstract: “Warming hiatus” occurred in the Altay-Sayan Mountain Region, Siberia in c. 1997–2014. We analyzed evergreen conifer (EGC) stands area (satellite data) and trees (Siberian pine, *Pinus sibirica* Du Tour, Siberian fir, *Abies sibirica* Ledeb.) growth increment (dendrochronology data) response to climate variables before and during the hiatus. During the hiatus, EGC area increased in the highlands (>1000 m) (+30%), whereas at low and middle elevations (<1000 m. a.s.l.) the EGC area decreased (-7%). The EGC area increase was observed on the rain-ward northwest slopes mainly. In highlands, EGC area increase mainly correlated with summer air temperature, whereas at low and middle elevations EGC area decrease correlated with drought index SPEI and vapor pressure deficit (VPD). EGC mortality (fir and Siberian pine) in lowland was caused by the synergy of water stress (inciting factor) and bark-beetle attacks (contributing factor). Tree growth increment (GI) dynamics differs with respect to elevation. At high elevation (1700 m) GI permanently increased since warming onset, whereas at the middle (900 m) and low elevations (450 m) GI increased until c. 1983 yr. with followed depression. That GI “breakpoint” occurred about a decade before hiatus

onset. In spite of growth depression, during hiatus GI was higher than that in pre-warming period. At high elevation, GI positively responded to elevated June temperatures and negatively to moisture increase (precipitation, root zone moisture content, VPD, and SPEI). At low elevation GI negatively responded to June temperatures and positively to moisture increase. For both, low and high elevation, these patterns persisted throughout the study period (1967–2014). On the contrary, at middle elevations GI dependence on climate variables switch after breakpoint year (1983). Before breakpoint, June air temperature (positive correlation) and moisture (negative correlations) controlled GI. Further temperature increase leads GI depression and switched correlation signs to opposite (from positive to negative with temperature, and from negative to positive with moisture variables).

Keywords: Growth increment; Warming hiatus; Warming impact; Conifer decline; Tree growth; Tree mortality; Conifer mortality; Water stress

Introduction

The effect of climate change on coniferous

Received: 06 June 2018
Revised: 12 October 2018
Accepted: 13 November 2018

forests, both positive and negative, was observed throughout the boreal zone (e.g., [Andregg et al. 2013](#); [Allen et al. 2015](#)). Deterioration of spruce (*Picea ajansis*) and fir (*Abies nephrolepis*) conditions were noticed in habitats of the Far East ([Man'ko et al. 1998](#)), *Abies sibirica* and *Pinus sibirica* in Baikal region and the Eastern Sayan and the Kuznetsk Alatau Mountains ([Kharuk 2013a, 2017b,c](#)).

Mortality of spruce (*Picea abies*) in the European part of Russia, in forests of eastern and Western Europe is associated with the deterioration of water condition ([Chuprov 2008](#); [Sarnatzkii 2012](#); [Haynes et al. 2014](#); [Kharuk et al. 2015](#)). Along with moisture-sensitive spruce, mortality of relatively drought tolerant *Pinus sylvestris* L. was observed in the forest-steppe zone of Ukraine and Belarus ([Lufarov and Kovalishin 2017](#)). Extensive conifers mortality has been reported in the forests of USA and Canada ([Millar and Stephenson 2015](#); [Kolb et al. 2016](#); [Hogg et al. 2017](#)). Alongside conifers, deciduous (*Populus tremuloides*, *Betula pendula*) also suffer from increased drought ([Michaelian et al. 2011](#); [Kharuk et al. 2013b](#)).

Besides climatic impact, forest mortality is also caused by the mass attacks of insects – bark beetles, xylophages, needle-eating pests ([Allen et al. 2010, 2015](#); [Kharuk et al. 2017b,c](#)). In particular, climate changes favored Siberian silkmoth (*Dendrolimus sibiricus* Tschetv.) northward migration ([Kharuk et al. 2017d](#)). Currently, one of the main factors of forests degradation are earlier “doze off” species, such as *Polygraphus proximus* Blandf. that have led to the mass mortality of *Abies sibirica* in Siberia ([Krivets et al. 2015](#); [Kharuk et al. 2017b](#)). In the North American forests, the synergy of water stress and insects resulted in tree mortality at an area measuring 25 million ha ([Coleman et al. 2014](#); [Millar and Stephenson 2015](#)).

Alongside negative impacts, climate change led to the upward and northward treeline shifts ([Devi et al. 2008](#); [Kharuk et al. 2010, 2017a](#); [Petrov et al. 2015](#)). Warming promotes “dark needle conifer” (*Abies sibirica*, *Pinus sibirica*, *Picea obovata*) migration into the zone of larch dominance ([Kharuk et al. 2005](#)), and evergreen conifers (EGC) density increase in some ecoregions ([He et al. 2017](#)). These positive impacts mainly referred to “accelerating warming” period (c. 1970th

– the end of 1990th). Meanwhile, controversial data are reported for the followed “hiatus” period, i.e. warming anomaly observed in 1998–2013, when air warming rate fell below long-term average warming rate ([Hartmann et al. 2013](#); [Medhaug et al. 2017](#)).

This study aims to analyze the EGC (mainly *Abies sibirica* L. and *Pinus sibirica* Du Tour) area dynamics in different elevational belts of the Altai-Sayan region (ASR) during warming hiatus. ASR, which includes the most part of the Altai-Sayan highland, is a priority ecoregion in the Asian continent ([Figure 1](#)). The mountainous terrain of ASR shapes considerable eco-climatic gradients by which mountain forests became a sensitive indicator of climate changes. These forests should experience noticeable distributional and compositional dynamics driven by changes in air temperature, water regime, and growing season length.

We hypothesized different EGC response to warming in different elevation belts with the modification effect of relief features. We are seeking the answers to the following questions: (a) What is the dynamics of EGC area in different elevation belts? (b) How do relief features (exposure, slope steepness) modify EGC area dynamics? (c) How do the EGC area and tree growth index respond to the climatic variables before and during hiatus?

1 Materials and Methods

1.1 Study area

The Altai-Sayan Region (ASR; [Figure 1](#)) has a total area of ~85 million hectares. The forested area is about 39 million ha, including ~7.7 million ha of evergreen conifers (MODIS satellite-derived estimates). Mountain relief prevails on the territory with the absolute height up to 4330 m a.s.l. The main types of forests are Siberian pine and fir (*Pinus sibirica*, *Abies sibirica*), fir and spruce (*Abies sibirica*, *Picea obovata*), pine (*Pinus sylvestris*) and larch (*Larix sibirica*) stands.

The climate is sharply continental with cold winters and cool summers. The average temperatures are -15°C ... -18°C in January, +10°C ... +14°C in July (in the foothills around

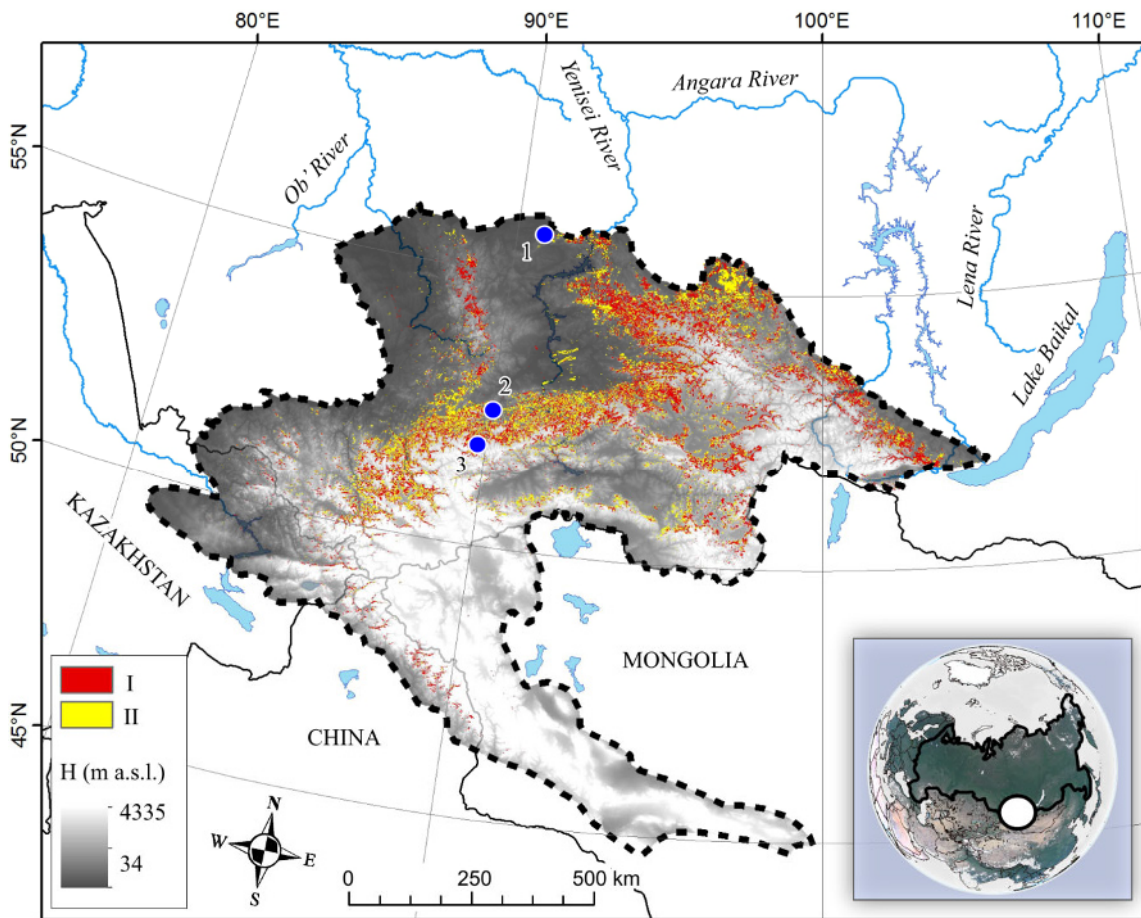


Figure 1 Sketch-map of the Altay-Sayan Region (ASR). Positive (I) and negative (II) trends in EGC areas are indicated by red and yellow, respectively. 1, 2, 3 – test sites within low (450 m a.s.l.), middle (900 m a.s.l.), and high (1700 m a.s.l.) elevations. H – elevation above sea level (m).

+19°C ... +20°C). The amount of precipitation on the windward slopes reaches 1200–2500 mm. The averages (2000–2017) for the region temperature and rainfall were -2°C (summer +15°C, winter -21°C) and 495 mm (summer – 215 mm, winter – 50 mm), respectively.

1.2 Materials

The dynamics of the EGC area was analyzed using MODIS products (on ground resolution 500m, period of 2001–2013; product MCD12Q1: https://lpdaac.usgs.gov/dataset_discovery/modis/modis_products_table/mcd12q1; Friedl et al. 2010). The burned areas were excluded from the analysis with the available MCD64A1 data (<http://modis-fire.umd.edu>). DEM GMTED2010 with on-ground resolution 250 m and elevation error 28 m (<https://lta.cr.usgs.gov/GMTED2010>) was used for geospatial analysis.

Dependences of EGC area and growth increment (GI) were analyzed with the main eco-climatic variables: air temperature, precipitation, vapor pressure deficit (VPD), drought index SPEI, root zone moisture content (RZMC), sum of active temperatures ($t \geq +5^\circ\text{C}$), and growth period length (the number of days with $t \geq +5^\circ\text{C}$). According to Rossi et al. (2008), in cold regions conifer cambium activity starts at temperatures of about of +4°C...+6°C. Temperature and precipitation data were drawn from the CRU TS 4.01 dataset (<https://crudata.uea.ac.uk/cru/data/hrg>; Harris and Jones 2017). The values of SPEI drought index were taken on the website <http://spei.csic.es> (spatial resolution $0.5^\circ \times 0.5^\circ$). SPEI is determined by the difference between precipitation and potential evapotranspiration (Vicente-Serrano et al. 2010). The vapor pressure deficit (VPD) was calculated based on CRU TS4.01 data using equations described in <https://crudata.uea.ac.uk/>

[~timm/grid/index-faq.html](#). The root zone moisture content and the number of days with the specified temperature were calculated with MERRA2 data (0.5° × 0.625° resolution, <https://gmao.gsfc.nasa.gov/reanalysis/MERRA-2>; Gelaro et al. 2017). The wood samples for dendrochronological analysis were taken using the increment borer at "breast height" level (1.3 m) during field studies in 2014–2016.

1.3 Methods

To assess the area maps of EGC density trends we used MCD12Q1 maps (the differences between the average values in 2011–2013 and 2001–2003). In the specified maps, according to IGBP classification, lands dominated by woody vegetation with a percent cover > 60% are referred to evergreen forests. Along with absolute, the normalized areas A_i were assumed as the ratio of an absolute area B_i to C_i area of i -elements of relief (Kharuk et al. 2010). The analysis algorithm included the following stages. (1) Creation of a burned area mask based on MCD64A1 data. (2) Filtration of burned areas. (3) Cutting a selected fragment of the territory and transforming it into Albers equal-area projection. (4) Formation of binary layers (EGC and background). (5) Assessment of maps for the initial (2001–2003) and final (2011–2013) periods assuming that EGC pixel is registered on the maps for the initial and final periods only if it was observed simultaneously on all images of the considered period. (6) Assessment of changes in EGC areas between the initial and final periods. (7) Calculation of area changes distribution for the relief features (elevation, exposure, slope steepness). (8) Calculation of EGC stands spatial density for each year using the method of focal statistics with averaging within a sliding window of 5 pixels. (9) Generation of a multilayer composite covering the entire analyzed period. (10) Calculation of linear trends for each pixel. The raster of trend lines slope coefficients, the significance levels of trends and the Pearson correlation coefficient were calculated. (11) Calculation of areas with statistically significant ($p < 0.05$) trends of EGC density. (12) Calculation of zones with statistically significant ($p < 0.05$) trends in climate variables. (13) Calculation of trends distribution for the relief features. The

algorithm is implemented using ESRI ArcGIS and Python script.

The dendrochronological analysis was carried out on the selected *Pinus sibirica* trees (at elevations of 1700 m and 900 m a.s.l., $N = 28$ and $N = 16$, respectively), and *Abies sibirica* trees (elevation 450 m a.s.l., $N = 123$). LINTAB 3 platform with precision 0.01 mm was used to measure wood cores (Rinn 1996). As a result, absolute individual tree-ring chronologies (in millimeters) were obtained. TSAP and COFECHA were used to assess the quality of crossdating and measurement accuracy (Holmes 1983). To eliminate the age trend, we applied the standardization procedure that converts the time series of the annual rings width to the time series of unitless indices with a defined mean of 1.0 and a relatively constant variance (Speer 2010).

2 Results

2.1 Climate variables dynamics

Climate variables strongly depend on the elevation gradient (Figure 2). Air temperature, length of growth season (the number of days with $t > 5^\circ\text{C}$) and RZMC decreasing with elevation increase; precipitation reaches its maximum at about 1200–1300 m a.s.l. with minimal values at low and high elevations. VPD has maximal values at low elevations (100–500 m a.s.l.; Figure 2).

At both, low and high elevations, “warming hiatus” was observed from 1997 till c. 2014. (Figures 3a, g). At high elevation, summer temperature during hiatus increased about $+1.0^\circ\text{C}$ in comparison with the “pre-warming” period (Figure 3g), besides there was found a 3-days increase in the length of the growing season (Figure 2l). At high elevations, minimal values trend followed precipitation increase in 1970th–80th. Precipitation trends were not observed at low elevations (Figure 3b).

2.2 Temporal and spatial dynamics of EGC area in Altai-Sayan Region (ASR)

During warming hiatus, the area of EGC increased by ~20%, nevertheless there was multidirectional dynamics along an elevation

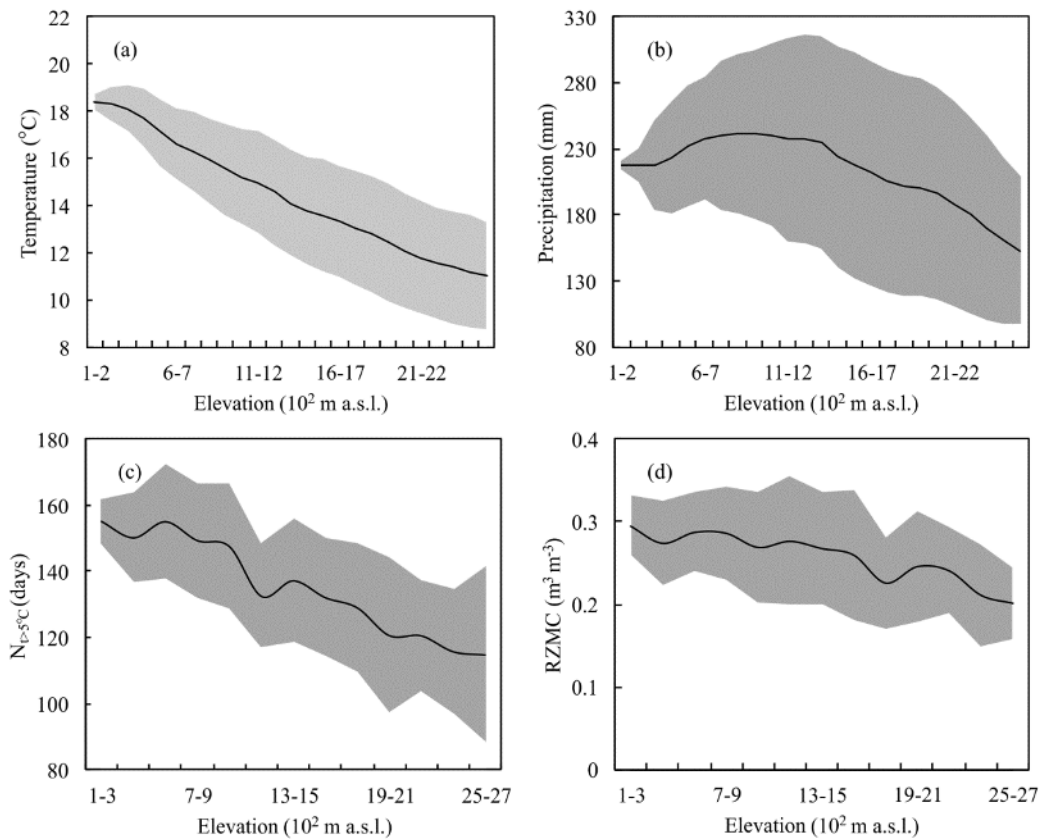


Figure 2 Distribution of eco-climatic variables across an elevation gradient (mean summer values for 2001–2013). (a) Temperature, (b) precipitation, (c) growth season (N days with $t > 5^{\circ}\text{C}$), (d) RZMC (root zone moisture content). Standard deviation indicated by grey.

gradient: at low and middle elevations (<1000 m a.s.l.) the area of EGC decreased (-7%), while in the highlands it increased ($+30\%$; [Figure 4a](#)). Negative and positive EGC trends covered 8% and 17% of the total area of EGC, respectively ([Figure 1](#)).

The main changes of EGC area observed along an elevation gradient ([Figure 4](#)) with the modified impact of exposure and slope steepness ([Figure 5](#)). Along an elevation gradient, EGC area changes (ΔS) switched from minus to plus at about 800 m a.s.l. ([Figure 4a](#)). Maximums of ΔS decrease and increase observed at 650 and 1450 m a.s.l., respectively. There are similarities in distributions of EGC area trends and drought index SPEI trends. Thus, forest mortality observed mainly within negative SPEI areas, whereas the EGC area increase corresponded to positive SPEI trends ([Figure 4b](#)). Similarly, within high VPD values (approx. <1000 m) mortality prevailed, whereas the zone of low VPD coincided with EGC area increase ([Figure 4c](#)).

As for slope steepness, maximal EGC area

increase was observed at slopes with about 10° , whereas there was a relative increase (in percentage points) with slope steepness increase ([Figure 5a](#)). As for exposure, EGC area decreased on the western slopes and increased on the northern ones ([Figure 5b,c](#)).

EGC area changes in lowlands correlated with mean summer temperature ($r = 0.64 \pm 0.06$; $p < 0.05$) and SPEI ($r = -0.64 \pm 0.07$; $p < 0.05$). In highlands EGC area correlated with total summer precipitation ($r = 0.67 \pm 0.08$; $p < 0.05$) and mean summer SPEI ($r = 0.64 \pm 0.07$; $p < 0.05$).

2.3 Dendrochronology data

Growth index analysis revealed different GI dynamics along an elevation gradient. In highlands, GI permanently increased since 1960th, whereas at middle and low elevations GI increased until 1983 (“breakpoint”) followed by growth depression ([Figure 6 a-c](#)).

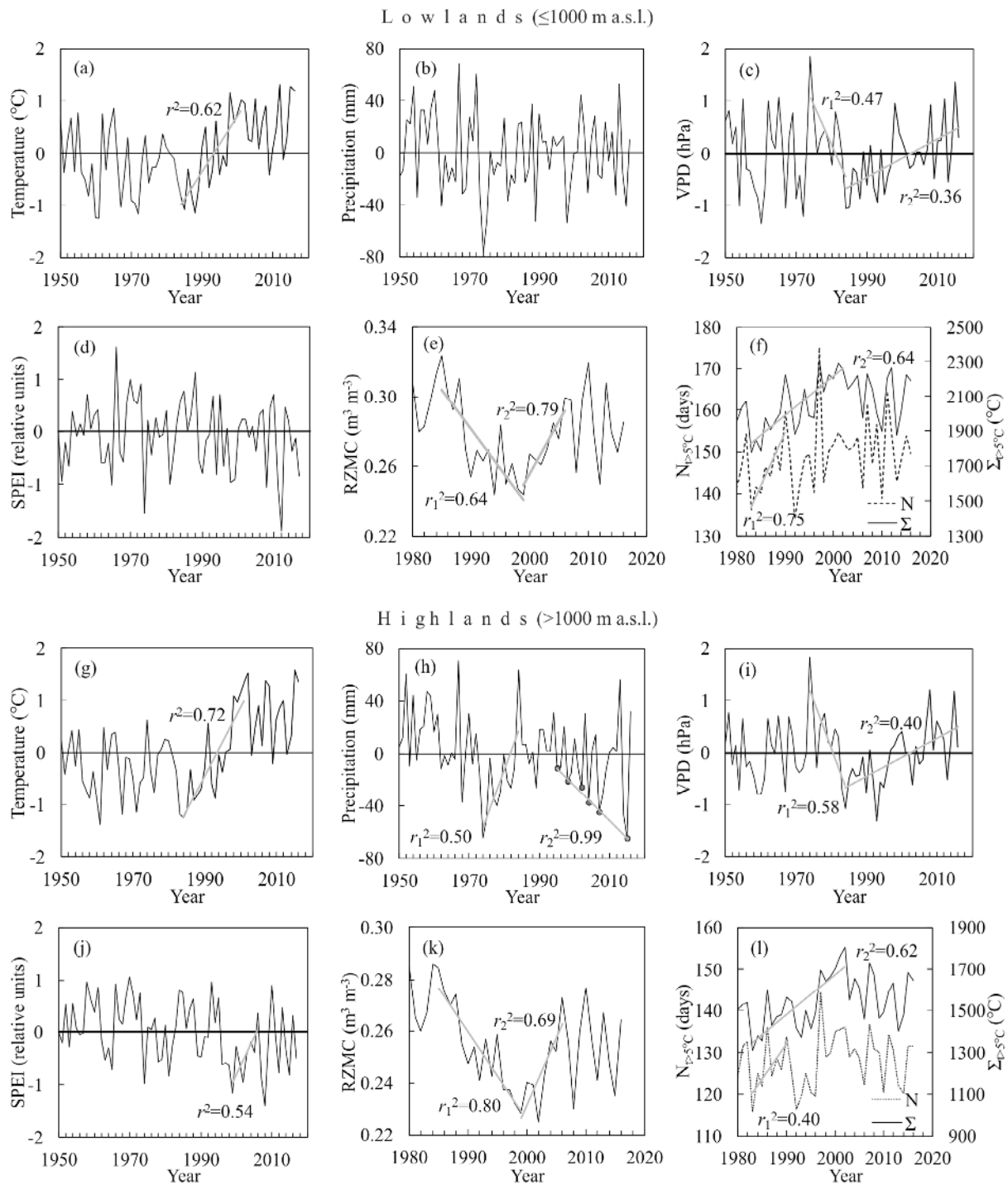


Figure 3 Dynamics of eco-climatic variables within the ASR for low (≤ 1000 , left columns) and high elevations (> 1000 m, right columns). (a, g) – summer temperature anomaly (base period 1950–2016), (b, h) – precipitation anomaly, (c, i) – VPD, (d, j) – SPEI, (e, k) – RZMC (root zone moisture content), (f, l) – number of days with $t > +5^{\circ}\text{C}$ [$N(t > 5^{\circ}\text{C})$] and sum of “active temperatures” [$\Sigma(t > 5^{\circ}\text{C})$]. Note: SPEI increase indicates drought decrease.

At low elevations, fir GI responded negatively to June temperature and VPD increases and positively to SPEI increase (Figure 7, Appendix 1). At middle elevation, Siberian pine GI response to climate variables switched at the breakpoint. Thus,

positive correlations with air temperature and VPD and negative with precipitation and SPEI switch to the opposite sign (Figure 7, Appendix 2).

At high elevations, GI positively correlated with air temperature and VPD and negatively with

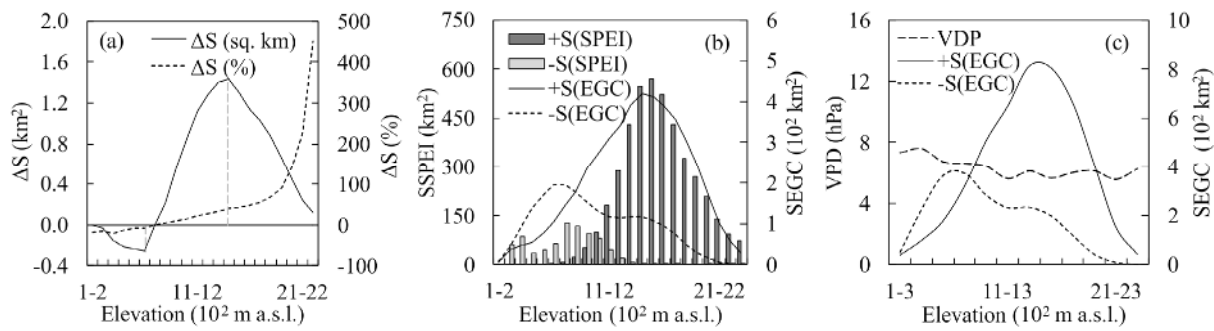


Figure 4 Distribution along elevation of (a) EGC area changes (ΔS), (b) trends of EGC and SPEI areas, and (c) VPD values. Symbols (+) and (-) indicate positive and negative trends, respectively. Dashed lines indicate maximums.

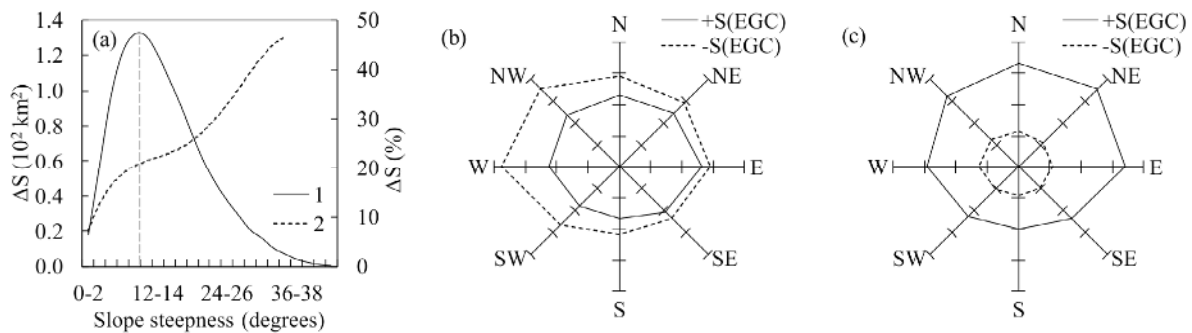


Figure 5 (a) EGC area changes (ΔS) relative to slope steepness. (b, c) EGC area trends dependence on exposure for elevations ≤ 1000 m a.s.l. (b) and > 1000 m a.s.l. (c), respectively.

precipitation (Figure 7a,b; Appendix 3). Correlations with root zone moisture content (RZMC) were negative at high elevation and positive at middle one (Figure 7b).

3 Discussion

In warming hiatus (1998–2013), in ASR (both at lowlands and highlands), there was no significant increase in air temperature and precipitation; moreover, there was a decrease in the sum of active temperatures (Figure 3l). Nevertheless, EGC area in the highlands increased (+30%), whereas in the lowlands (< 1000 m a.s.l.) area decreased (-7%).

That EGC area increase could be attributed to the higher air temperature ($+1.0^{\circ}\text{C}$) during hiatus than in the pre-warming period (1950–1970). Moreover, growing season length also increased (+3 days). Thus, during hiatus EGC stand's area in highlands was increasing due to improved thermal conditions on the background of sufficient precipitation. Similarly, He et al. (2017) found that evergreen conifer forest expansion in Western Siberia continued during warming hiatus. EGC

area increase attributed mainly to the growth of pre-existing small trees and seedlings because observations period (17 yr.) is too short for area expansion due to new trees establishment. For example, regeneration line upward shift estimated as 0.35–0.8 m/yr. (Kharuk et al. 2010, 2017a), or about 10–15 m for the observation period; that difference is hardly detectable by MODIS sensor.

Tree growth index in highlands also permanently increased since warming onset and during hiatus, whereas in lowlands initial GI positive response to warming switched to GI depression with a breakpoint in 1983 yr., more than a decade before hiatus onset (1997). Growth depression was caused by water stress via elevating air temperature. Meanwhile, highlands remained the zone of excessive moistening, which indicated negative correlations of GI with precipitation and root zone moisture content (and positive with VPD). At low and middle elevations (< 1000 m), on the contrary, hiatus coincided with EGC area decrease (fir and Siberian pine stands areas; Kharuk et al. 2017b,c). These areas mainly refer to the zones of decreased moistening (as indicated by SPEI and VPD values; Figure 3c, d). Periods of EGC area decrease and GI depression coincided (Figure 6a, b).

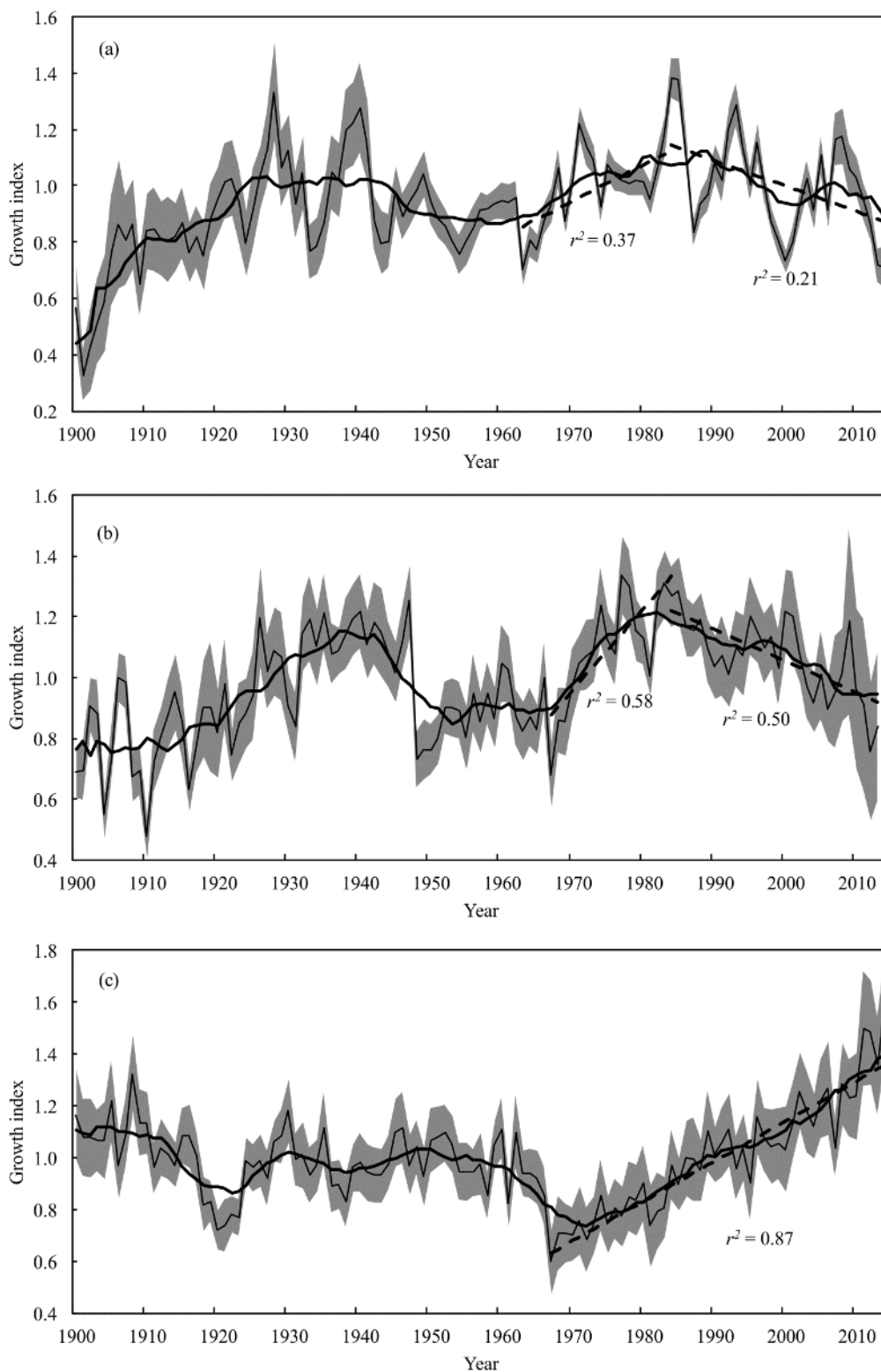


Figure 6 Growth increment (GI) dynamics of fir (a; elevation 450 m a.s.l.), and Siberian pine (b, c: 900 m and 1700 m a.s.l.). Dense line: data filtered by 11 yr. window. Gray background: $p > 0.05$.

Similarly, observations in Southern Tibet, China showed that while *Abies georgei* population is expanding and upper limit of this species has advanced upslope, the lowest limit has retreated

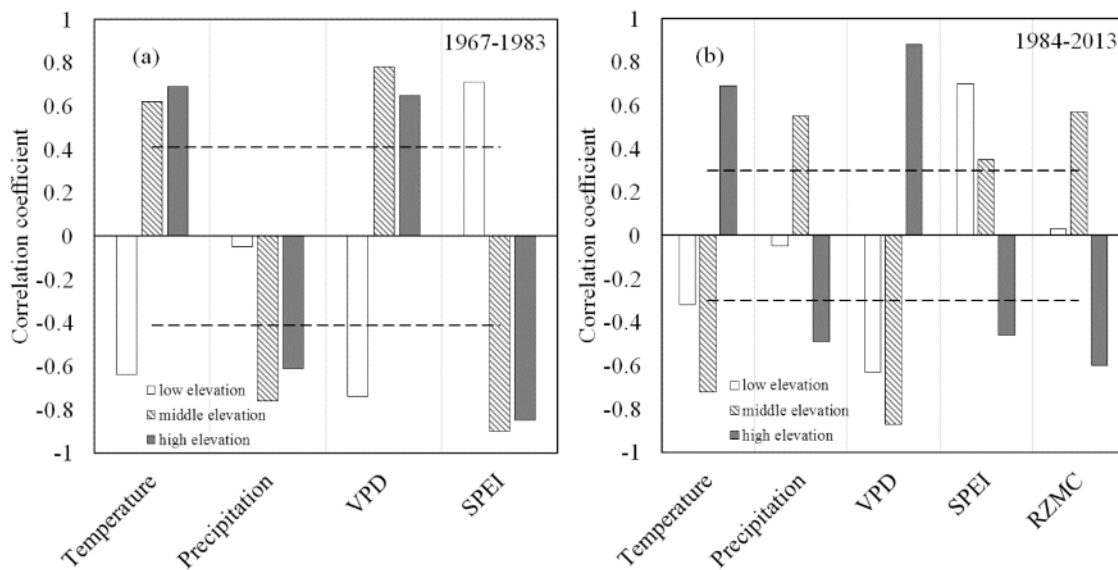


Figure 7 Correlations between growth increment (GI) and climate variables before (1967–1983) and after (1984–2013) GI breakpoint for low (450 m), middle (900), and high (1700) elevation. Variables: June temperature, May–August precipitation, June–August VPD (vapor pressure deficit), May–August SPEI, July–August RZMC (root zone moisture content). Dashed lines indicate correlation with $p = 0.05$.

upslope (Wong et al. 2013; Shen et al. 2016).

At the middle elevations, the “growth limitation switch” was observed in the mid of 1980th, when temperature limitation switched to moisture limitation. Thus, since warming onset GI correlated positively with air temperature and negatively with precipitation, whereas during growth depression sign of these correlations switched. Similar switch (from temperature to moisture limitation) was described for *Pinus mugo* at high Alps (Churakova et al. 2016).

Notably, GI patterns at low and middle elevations are typical for water-stressed declining stands and may precede stands mortality (Cailleret et al. 2017). Within study area taiga mortality (mainly Siberian pine and fir; Appendixes 4, 5) was caused by water stress in synergy with bark-beetles attacks (Kharuk et al. 2016). Earlier Siberian pine and fir decline and mortality described within middle (500–900 m a.s.l.) elevations in the ASR north (Kuznetsk Alatau and East Sayan Mountains; Kharuk et al. 2013a, 2017b). As for fir mortality, the most hazardous pest is *Polygraphus proximus*, the bark-beetle that was not observed before warming (Krivecz et al. 2015). Similarly, increased water deficit together with pest attacks caused Douglas fir growth decrease in western US forests (Restaino et al. 2016).

Projected air temperature increase (IPCC 2014)

will lead further fir and Siberian pine area reduction in the lowlands, and area increase the highlands, as well as trees migration into alpine tundra. Moreover, warming will also adversely affect wildfire regime; thus, both fire frequency and burned area in Siberia increased in recent decades (Kharuk and Ponomarev 2017e). An additional factor of tree mortality is an activation of primary pests such as Siberian silkmoth (*Dendrolimus sibiricus*), which extended its range northward and caused huge forest decline and mortality (on about 800 thousand ha) in mid-taiga zone (Kharuk et al. 2017d).

4 Conclusions

Warming hiatus in ASR caused a general increase in the EGC area (+20% mean). However, at lowlands (<1000 m a.s.l.) EGC area decreased (-7%) with significant (+30%) increase at high elevations (>1000 m). EGC area increase were mainly observed on the rain-ward northwest slopes. EGC area increase in highlands correlated with air temperature mainly, whereas EGC area decreases in lowlands correlated with drought index SPEI and VPD.

Tree mortality in lowlands was caused by increased water stress via elevated temperature in

synergy with bark-beetles attacks.

Tree GI dynamics was determined by water regime. Within the zone of sufficient precipitation (highlands) GI demonstrates permanent increase since warming onset, whereas at low and middle elevation initial positive GI response to elevating temperature switched to growth depression (with a breakpoint at 1983 yr.). At the middle elevations, “GI - climate variables” correlations changed signs after breakpoint (from plus to minus with temperature and VPD, and from minus to plus with precipitation and SPEI).

References

- Allen CD, Macalady AK, Chenchouni H, et al. (2010) A global overview of drought and heat-induced tree mortality reveals emerging climate change risks for forests. *Forest Ecology and Management* 259(4): 660-684. <https://doi.org/10.1016/j.foreco.2009.09.001>
- Allen CD, Breshears DD, McDowell NG (2015) On underestimation of global vulnerability to tree mortality and forest die-off from hotter drought in the Anthropocene. *Ecosphere* 6(8): 129. <https://doi.org/10.1890/ES15-00203.1>
- Andregg LDL, Andregg WRL, Berry JA (2013) Not all droughts are created equal: translating meteorological drought into woody plant mortality. *Tree Physiology Review* 33(7): 701-712. <https://doi.org/10.1093/treephys/tpo044>
- Cailleret M, Jansen S, Robert EMR, et al. (2017) A synthesis of radial growth patterns emerging tree mortality. *Global Change Biology* 23 (4): 1675-1690. <https://doi.org/10.1111/gcb.13535>
- Chuprov NP (2008) About the problem of spruce decay in the European North of Russia. *Russian Forestry* 1: 24-26. (In Russian)
- Coleman TW, Jones MI, Courtial B, et al. (2014) Impact of the first recorded outbreak of the Douglas-fir tussock moth, *Orgyia pseudotsugata*, in southern California and the extent of its distribution in the Pacific Southwest region. *Forest Ecology and Management* 329: 295-305. <https://doi.org/10.1016/j.foreco.2014.06.027>
- Devi N, Hagedorn F, Moiseev P, et al. (2008) Expanding forests and changing growth forms of Siberian larch at the Polar Urals treeline during the 20th century. *Global Change Biology* 14(7): 1581-1591. <https://doi.org/10.1111/j.1365-2486.2008.01583.x>
- Friedl MA, Sulla-Menasha D, Tan B, et al. (2010) MODIS Collection 5 global land cover: Algorithm refinements and characterization of new datasets. *Remote Sensing of Environment* 114: 168-182. <https://doi.org/10.1016/j.rse.2009.08.016>
- Gelaro R, McCarty W, Suárez MJ, et al. (2017) The Modern-Era Retrospective Analysis for Research and Applications, Version 2 (MERRA-2). *Journal of Climate* 30: 5419-5454. <https://doi.org/10.1175/JCLI-D-16-0758.1>
- Churakova SO, Saurer M, Bryukhanova MV, et al. (2016) Site-specific water-use strategies of mountain pine and larch to cope with recent climate change. *Tree Physiology* 36: 942-953. <https://doi.org/10.1093/treephys/tpw060>
- Hartmann DL, Klein Tank AMG, Rusticucci M, et al. (2013) Observations: Atmosphere and Surface. In: Stocker TF, Qin D, et al. (eds.), *Climate Change 2013: The Physical Science Basis*. Contribution of Working Group I to the Fifth Assessment Report of the Intergovernmental Panel on Climate Change. Cambridge University Press, Cambridge, United Kingdom and New York, NY, USA.
- Harris IC, Jones PD (2017) CRU TS4.01: University of East Anglia Climatic Research Unit; Climatic Research Unit (CRU) Time-Series (TS) version 4.01 of high-resolution gridded data of month-by-month variation in climate (Jan. 1901–Dec. 2016). Centre for Environmental Data Analysis, 04 December 2017. <https://doi.org/10.5285/58a8802721c94c66ae45c3baa4d814do>
- Haynes KJ, Allstadt A, Klimetzek D (2014) Forest defoliator outbreaks under climate change: Effects on the frequency and severity of outbreaks of five pine insect pests. *Global Change Biology* 20: 2004-2018. <https://doi.org/10.1111/gcb.12506>
- He Y, Huang J, Shugart HH, et al. (2017) Unexpected evergreen expansion in the Siberian forest under warming hiatus. *Journal of Climate* 30: 5021-5039. <https://doi.org/10.1175/JCLI-D-16-0196.1>
- Holmes RL (1983) Computer-assisted quality control in tree-ring dating and measurement. *Tree-Ring Bulletin* 43: 69-78.
- Hogg EH, Michaelian M, Hook TI, Undershultz ME (2017) Recent climatic drying leads to age - independent growth reductions of white spruce stands in western Canada. *Global Change Biology* 23(12): 5297-5308. <https://doi.org/10.1111/gcb.13795>
- IPCC (2014) *Climate Change 2014: Impacts, Adaptation, and Vulnerability*. A Contribution of Working Group II to the Fifth Assessment Report of the Intergovernmental Panel on Climate Change. In: Field CB, Barros VR, et al. (eds.), *World Meteorological Organization*, Geneva, Switzerland. p 190. Available online: <http://www.ipcc.ch/report/ar5/wg2/>, accessed on 19 May 2017.
- Kharuk VI, Dvinskaya ML, Ranson KJ, Im ST (2005) Expansion of Evergreen Conifers to the Larch-Dominated Zone and Climatic Trends. *Russian Journal of Ecology* 36(3): 164-170. <https://doi.org/10.1007/s11184-005-0055-5>
- Kharuk VI, Ranson KJ, Im ST, Vdovin AS (2010) Spatial distribution and temporal dynamics of high-elevation forest stands in southern Siberia. *Global Ecology and Biogeography* 19: 822-830. <https://doi.org/10.1111/j.1466-8238.2010.00555.x>
- Kharuk VI, Im ST, Oskorbin PA, et al. (2013a) Siberian pine decline and mortality in southern Siberian mountains. *Forest Ecology and Management* 310: 312-320. <https://doi.org/10.1016/j.foreco.2013.08.042>
- Kharuk VI, Ranson KJ, Oskorbin PA, Im ST, Dvinskaya ML (2013b) Climate induced birch mortality in Trans-Baikal lake region, Siberia. *Forest Ecology and Management* 289: 385-392. <https://doi.org/10.1016/j.foreco.2012.10.024>
- Kharuk VI, Im ST, Dvinskaya ML, et al. (2015) Climate-induced

Acknowledgements

This research was supported by the Russian Foundation for Basic Research (grants #18-05-00432). Dendrochronological analysis was supported by the Russian Science Foundation (17-74-10113).

Electronic supplementary material: Supplementary material (Appendixes 1-5) is available in the online version of this article at <https://doi.org/10.1007/s11629-018-5071-6>

- mortality of spruce stands in Belarus. *Environmental Research Letters* 10: 125006. <https://doi.org/10.1088/1748-9326/10/12/125006>
- Kharuk VI, Demidko DA, Fedotova EV, et al. (2016) Spatial and temporal dynamics of Siberian silk moth large-scale outbreak in dark-needle coniferous tree stands in Altai. *Contemporary Problems of Ecology* 9: 711-720. <https://doi.org/10.1134/S199542551606007X>
- Kharuk VI, Im ST, Dvinskaya ML, et al. (2017a) Tree wave migration across an elevation gradient in the Altai Mountains, Siberia. *Journal of Mountain Science* 14(3): 442-452. <https://doi.org/10.1007/s11629-016-4286-7>
- Kharuk VI, Im ST, Petrov IA, et al. (2017b) Fir decline and mortality in the southern Siberian Mountains. *Regional Environmental Change* 17: 803-812. <https://doi.org/10.1007/s10113-016-1073-5>
- Kharuk VI, Im ST, Petrov IA, et al. (2017c) Climate-induced mortality of Siberian pine and fir in the Lake Baikal Watershed, Siberia. *Forest Ecology and Management* 384: 191-199. <https://doi.org/10.1016/j.foreco.2016.10.050>
- Kharuk VI, Im ST, Ranson KJ, Yagunov MN (2017d) Climate-Induced Northerly Expansion of Siberian Silkmoth Range. *Forests* 8(8): 301. <https://doi.org/10.3390/f8080301>
- Kharuk VI, Ponomarev EI (2017e) Spatiotemporal characteristics of wildfire frequency and relative area burned in larch-dominated forests of Central Siberia. *Russian Journal of Ecology* 48(6): 507-512. <https://doi.org/10.1134/S1067413617060042>
- Kolb TE, Fettig CJ, Ayres MP, et al. (2016) Observed and anticipated impacts of drought on forests insects and diseases in the United States. *Forest Ecology and Management* 380: 321-324. <https://doi.org/10.1016/j.foreco.2016.04.051>
- Krivecz SA, Kerchev IA, Bisirova EM, et al. (2015) Expansion of four-eyed fir bark beetle *Polygraphus proximus* blandf. (coleoptera, curculionidae: colytinae) in Siberia. *Issues of the Saint-Petersburg forest-technical academy* 211: 33-45. (In Russian)
- Luferov AO, Kovalishin VR (2017) Problem of mortality of pine stands on the territory of Belarus and Ukraine woodlands. Materials of the fifth international conference-meeting "Preservation of forest genetic resources". 2-7 October 2017, Gomel, Belarus. Belarus Institute of forest NAN, "Kolordryg" publishing, pp 119-120. (In Russian)
- Man'ko YI, Gladkova GA, Butovets GN, Norihiza Kamibayasi (1998) Monitoring of fir-spruce forests decay in the Central Sikhote-Alin. *Russian Forest Sciences* 1: 3-16. (In Russian)
- Medhaug I, Stolpe MB, Fischer EM, Knutti R (2017) Reconciling controversies about the global warming hiatus. *Nature* 545: 41-47. <https://doi.org/10.1038/nature22315>
- Michaelian M, Hogg EH, Hall RJ, Arsenault E (2011) Massive mortality of aspen following severe drought along the southern edge of the Canadian boreal forest. *Global Change Biology* 17(6): 2084-2094. <https://doi.org/10.1111/j.1365-2486.2010.02357.x>
- Millar CI, Stephenson NL (2015) Temperate forest health in an era of emerging megadisturbance. *Science* 349(6250): 823-826. <https://doi.org/10.1126/science.aaa9933>
- Petrov IA, Kharuk VI, Dvinskaya ML, Im ST (2015) Reaction of Coniferous Trees in the Kuznetsk Alatau Alpine Forest-Tundra Ecotone to Climate Change. *Contemporary Problems of Ecology* 8(4): 423-430. <https://doi.org/10.1134/S1995425515040137>
- Rinn F (1996) Tsap V 3.6. Reference manual: computer program for tree-ring analysis and presentation. Heidelberg, Germany
- Restaino CM, Peterson DL, Littell J (2016) Increased water deficit decreases Douglas fir growth throughout western US forests. *Proceedings of the National Academy of Sciences* 113(34):9557-562. <https://doi.org/10.1073/pnas.1602384113>
- Rossi S, Deslauriers A, Gričar J, et al. (2008) Critical temperatures for xylogenesis in conifers of cold climates. *Global Ecology and Biogeography* 17: 696-707. <https://doi.org/10.1111/j.1466-8238.2008.00417.x>
- Sarnatezkii VV (2012) Zonal-typological patterns of periodic large-scale spruce decay in Belarus. *Proceedings of BGTU. Forest estate*. pp 274-276. (In Russian)
- Shen ZQ, Lu J, Hua M, Fang JP (2016) Spatial pattern analysis and associations of different growth stages of populations of *Abies georgei* var. *smithii* in Southeast Tibet, China. *Journal of Mountain Science* 13(12): 2170-2181. <https://doi.org/10.1007/s11629-016-3849-y>
- Speer JH (2010) *Fundamentals of Tree-Ring Research*. University of Arizona Press. p 368.
- Vicente-Serrano SM, Beguería S, López-Moreno JI (2010) A Multi-scalar drought index sensitive to global warming: The Standardized Precipitation Evapotranspiration Index - SPEI. *Journal of Climate* 23: 1696-1718. <https://doi.org/10.1175/2009JCLI2909.1>
- Wong MHG, Duan CQ, Long YC, et al. (2013) How will the distribution and size of subalpine *Abies georgei* forest respond to climate change? A study in Northwest Yunnan, China. *Physical Geography* 31(4): 319-335. <https://doi.org/10.2747/0272-3646.31.4.319>